On the Nature and Structure of a New MoVTeO Crystalline Phase

E. García-González,*,† J. M. López Nieto,*,‡ P. Botella,‡ and J. M. González-Calbet†

Departamento Química Inorgánica, Facultad de Ciencias Químicas, Universidad Complutense Madrid, 28040 Madrid, Spain, and Instituto de Tecnología Química, UPV−CSIC, Avenida de los Naranjos s/n, 46022 Valencia, Spain

Received June 3, 2002. Revised Manuscript Received July 29, 2002

A new MoVTeO mixed oxide has been obtained during the calcination of the corresponding catalyst precursor mixture at 600 °C in N_2. The crystal structure has been studied by means of X-ray diffraction, electron diffraction, high-resolution electron microscopy, and diffuse reflectance spectroscopy. Its XRD pattern, similar to those observed in hexagonal tungsten bronze (HTB) $K_{0.13-0.33}WO_3$, was indexed on the basis of a hexagonal cell of parameters a = 0.727 nm and c = 0.4012 nm. However, the electron microscopy study reveals the crystals as being formed by structural domains of an orthorhombically distorted unit cell derived from the HTB structure. Microstructural details are discussed in terms of tellurium location inside the hexagonal tunnels of the structure. The results obtained constitute the first step for elucidating the role of this new orthorhombic phase in the effectiveness of Mo−V−Te−Nb mixed oxide catalysts.

Introduction

Acrylonitrile and acrylic acid are two important intermediates for the preparation of fibers, synthetic rubbers, synthetic resins, and so forth.[1] Both are actually produced by gas-phase ammoxidation and oxidation of propylene, respectively. The trend in the coming years will be to replace it by propane, a less expensive raw material.

Mo−V−Te−Nb oxides have been proposed as one of the best catalysts in both the ammoxidation[2] and the selective oxidation[3] of propane, with yield to desired products near 50%. The catalyst preparation method, the optimal chemical composition, and the nature of the active and selective sites is still under discussion and research.[2−8] However, the main papers and patents published in recent years suggest the presence of at least two crystalline phases, although their structures are not well-resolved.

Two crystalline phases, namely, phase-M1 (with possible specific diffraction angles at 2θ (°) = 9.0, 22.1, 27.3, 29.2, and 35.4) and phase-M2 (with specific diffraction angles at 2θ (°) = 22.1, 28.2, 36.2, 45.2, and 50.0) were initially proposed to be present in active and selective catalysts for propane ammoxidation.[4] Similar crystalline phases could also be proposed in selective catalysts for the oxidation of propane to acrylic acid.[7,8] Recently, it has been suggested that the stoichiometry of these phases could correspond to $Te_{0.33}MO_3$ and $Te_{0.2}MO_{3.2}$ (with M = Mo, V, and Nb).[6] However, the resolution of these crystalline structures was carried out from a mixed metal oxide catalyst instead of from a pure crystalline phase.

Several crystalline phases have been reported in the Mo−V−Te−O system, which depend on the chemical composition, the preparation procedure, or calcination conditions.[9−13] From all of these, $TeMo_5O_{16}$ (a Mo-partially reduced telluromolybdate[14,15]) appears to be involved in selective MoVTeNb-based catalysts.[6−8]

Recently, the synthesis of new MoVTeO and MoVTeNbO mixed oxides with stoichiometry Te_xMO_z (x = 0.33−0.4; M = Mo and V or Mo, V, and Nb)[16] has been reported, which present XRD patterns similar to that

* To whom correspondence should be addressed. E-mails: esterg@ucmail.ucm.es; jmlopez@itq.upv.es.
† Universidad Complutense Madrid.
‡ UPV−CSIC.

(1) *Kirk−Othmer's Encyclopedia of Chemical Technology*, 14th ed.; Kirk, R. E., Othmer, F., Kroschwitz, J. I., and Howe-Grant, M., Eds.; John Wiley & Sons: New York, 1991.
(2) Ushikubo, T.; Nakamura, H.; Koyasu, Y.; Wajiki, S. U.S. Patent 5,380,933, 1995; EP 0 608 838 B1, 1997.
(3) Ushikubo, T.; Sawaki, I.; Oshima, K.; Inumaru, K.; Kovayakawa, S.; Kiyono, K. EP 0 603 836, 1993; U.S. Patent 5,422,328, 1993.
(4) Ushikubo, T.; Oshima, K.; Kayou A.; Hatano, M. *Stud. Surf. Sci Catal.* **1997**, *112*, 473.
(5) Asakura, K.; Nakatani, K.; Kubota T.; Iwasawa, Y. *J. Catal.* **2000**, *194*, 309.
(6) Aouine, M.; Dubois J. L.; Millet, J. M. M. *Chem. Commun.* **2001**, 1180.
(7) Lin, M.; Desai, T. B.; Kaiser, F. W.; Klugherz, P. D. *Catal. Today* **2000**, *61*, 223.
(8) Botella, P.; López Nieto, J. M.; Martinez-Arias A.; Solsona, B. *Catal. Lett.* **2001**, *74*, 149.
(9) Bart, J. C. J.; Petrini, G.; Giordano, N. *Z. Anorg. Allg. Chem.* **1975**, *413*, 180.
(10) Bart, J. C. J.; Petrini, G.; Giordano, N. *Z. Anorg. Allg. Chem.* **1975**, *412*, 258.
(11) Petrini, G.; Bart, J. C.J. *Z. Anorg. Allg. Chem.* **1981**, *474*, 229.
(12) Dimitriev, Y.; Bart, J. C. J.; Dimitrov, V.; Arnaudov, M. *Z. Anorg. Allg. Chem.* **1981**, *479*, 229.
(13) Sloczynski, J.; Sliva, B. *Z. Anorg. Allg. Chem.* **1978**, *438*, 295.
(14) Vallar, S.; Goreaud, M. *J. Solid State Chem.* **1997**, 129, 303.
(15) Forestier, P.; Goreaud, M. *C. R. Acad. Sci. Paris* **1991**, *312 (Ser. II)*, 1141.
(16) Botella, P.; López Nieto, J. M.; Solsona, B. *Catal. Lett.* **2002**, *78*, 383.

10.1021/cm021223m CCC: $22.00
Published on Web 09/19/2002

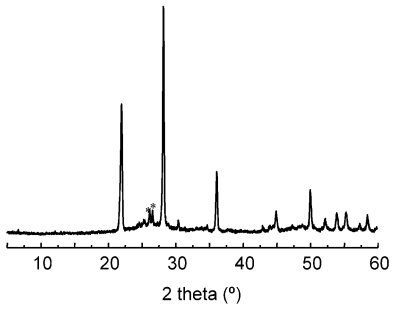

Figure 1. XRD pattern for $Te_{0.33}Mo_{0.75}V_{0.25}O_x$ (* diffraction maxima corresponding to $TeMo_5O_{16}$).

observed for $Sb_4Mo_{10}O_{31}$. These mixed metal oxides could be one of the crystalline phases detected in MoVTeNb-based catalysts. In this way, it has been observed that these new MoVTeO and MoVTeNb oxides are active phases in the oxidation of propene to acrolein and/or acrylic acid but are inactive in the partial oxidation of propane. However, their structures are still unsolved.

In this paper we present, for the first time, a structural investigation on a new MoVTeO bronze. The crystal structure has been determined by means of X-ray diffraction, electron diffraction, and high-resolution electron microscopy. Diffuse reflectance experiments have also been used to determine the oxidation state of each element.

Experimental Section

Samples were prepared by evaporation of an aqueous slurry comprising ammonium heptamolybdate, $(NH_4)_6Mo_7O_{24}{\cdot}4H_2O$ (Merck), telluric acid, $Te(OH)_6$ (Aldrich), and vanadyl sulfate, $VOSO_4$ (Aldrich). The slurry was evaporated in a rotavapor at 70 °C and 27 kPa and then dried at 100 °C overnight. The dried solid was heated in N_2 (100 mL/min) at 4 °C/min to 600 °C and then held at that temperature for 2 h. Finally, the sample was cooled in N_2 to room temperature. A black solid was obtained.

Powder X-ray diffraction (XRD) was performed on a Philips X'Pert diffractometer equipped with a graphite monochromator, operating at 40 kV and 45 mA and employing nickel-filtered Cu Kα radiation ($\lambda = 0.1542$ nm).

The total amount of molybdenum, vanadium, and tellurium was determined by EDS X-ray microanalysis carried out on both a JEOL 2000FX electron microscope supplied with a LINK analyzer AN10000 and a PHILIPS CM20FEG Super Twin electron microscope supplied with an EDAX analyzer DX-4 (resolution ≈135 eV and Super Ultra Thin Window).

Diffuse reflectance (DR) UV−vis spectra were collected on a Cary 5 equipped with a "Praying Mantis" attachment from Harric. Different reference compounds, such as V_2O_5, MgV_2O_6, $VOSO_4$, TeO_2, MoO_3, and $TeMo_5O_{16}$ were used.

Selected area electron diffraction (SAED) was carried out on a JEOL 2000FX electron microscope. High-resolution electron microscopy (HREM) was performed on both a JEOL 4000EX and PHILIPS CM20 FEG Super Twin electron microscopes. The samples for electron microscopy were ultrasonically dispersed in *n*-butanol and transferred to carbon-coated copper grids.

Results and Discussion

The calcined sample was first characterized by powder X-ray diffraction (Figure 1). The corresponding pattern was indexed on the basis of a hexagonal cell of parameters $a = 0.727(3)$ nm and $c = 0.4012(2)$ nm. It showed great similarity with the diffraction pattern of a HTB (hexagonal tungsten bronze) $K_{0.13-0.33}WO_3$[17] or $Sb_{0.4}MoO_{3.1}$.[18]

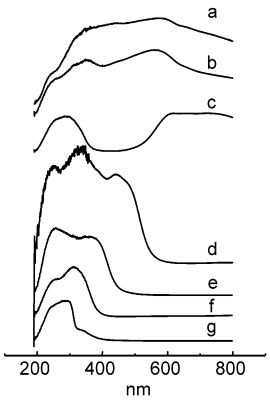

Figure 2. Diffuse reflectance UV−vis spectrum of $Te_{0.33}Mo_{0.75}V_{0.25}O_x$ (a). DR spectra of the reference compounds, $TeMo_5O_{16}$ (b), $VOSO_4$ (c), V_2O_5 (d), MgV_2O_6 (e), MoO_3 (f), and TeO_2 (g).

Some extra reflections were also observed as impurities. These can be related to the presence of a small amount of $TeMo_5O_{16}$ (JCPDS-31−874).

The chemical analysis of the crystals has been performed by means of EDS X-ray microanalysis. The Te/M (M = Mo + V) atomic ratio of 0.33 ± 0.01 was found in all the crystals investigated. However, the Mo/V atomic ratio slightly changed from crystal to crystal, but it was always close to 0.75/0.25. These results would lead to the composition $Te_{0.33}Mo_{0.75}V_{0.25}O_x$, which corresponds to that of the hexagonal bronze-type structure built up from Mo/V−O corner-sharing octahedra forming hexagonal channels that should be completely filled by the Te atoms.

Figure 2 shows the DR spectrum of $Te_{0.33}Mo_{0.75}V_{0.25}O_x$ (Figure 2a). For comparison, different reference compounds such as $TeMo_5O_{16}$, $VOSO_4$, V_2O_5, MgV_2O_6, MoO_3, and TeO_2 (Figure 2, spectra b−g) have been used.

Spectra corresponding to $Te_{0.33}Mo_{0.75}V_{0.25}O_x$ and $TeMo_5O_{16}$ show great similarity, although the former presents a band in the 350−450-nm region and the band at 550 nm in $TeMo_5O_{16}$ shifts to 580 nm in $Te_{0.33}Mo_{0.75}V_{0.25}O_x$. The absorption in the 400−450-nm region should be related to the presence of V^{5+} cations in octahedral coordination while the band in the 500−600-nm region may be assigned to Mo cations with an oxidation state lower than 6+.

It has been observed that the band in the 500−600-nm region shifts gradually with changes in the oxidation state of Mo. Thus, a band at 500 nm is observed in MoO_2 while this appears at 585 nm in Mo_9O_{26}.[9] The same trend has been reported in Mo−Te oxides: 550 nm in $TeMo_5O_{16}$[19] and 565 nm in $TeMo_4O_{13}$.[9] When considering the linear relation of observed band frequencies of intermediate molybdenum oxides as a function of the number of 4d electrons per cation,[20] it leads one to estimate the presence of 20% of Mo atoms with an

(17) Magnelli, A. *Acta Chem. Scand.* **1953**, *7*, 315.
(18) Parmentier, M.; Gleitzer, G.; Tilley, R. J. D. *J. Solid State Chem.* **1989**, *31*, 305.
(19) Bart, J. C. J.; Cariati, F.; Sgamellotti, A. *Inorg. Chim. Acta* **1979**, *36*, 105.
(20) Porter, V. R.; White, W. B.; Roy, R. *J. Solid State Chem.* **1972**, *4*, 250.

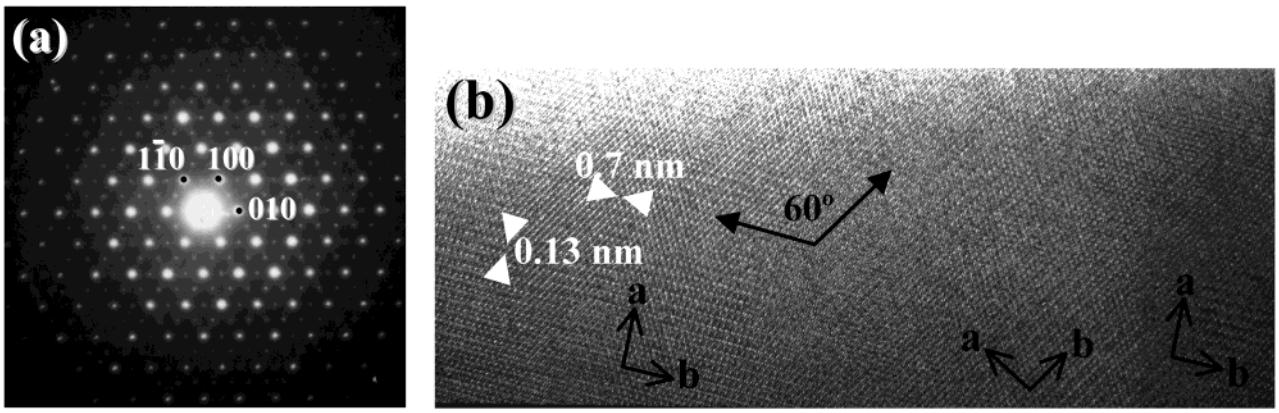

Figure 3. (a) SAED pattern taken along the [001] zone axis (Miller indices are assigned for hexagonal symmetry). (b) Corresponding high-resolution micrograph.

oxidation state of Mo^{5+} in $Te_{0.33}Mo_{0.75}V_{0.25}O_x$ (band at 580 nm) instead of 30% proposed in $TeMo_5O_{16}$ (band at 550 nm).[19]

On the other hand, the band in the 350−450-nm region can be related to VO_6 octahedra in different structural arrangements.[21] In this way, a shift from 358 to 450 nm can be observed for VO_6 octahedra in MgV_2O_6 (Figure 2e) and V_2O_5 (Figure 2d), respectively. Since MgV_2O_6 is characterized by the presence of highly distorted VO_6 octahedra (sharing edges and connected together through MgO_6 octahedra) as in V_2O_5, the different positions of the corresponding DR band could be related to the different V environments. According to this, vanadium atoms in $Te_{0.33}Mo_{0.75}V_{0.25}O_x$ should possess a distorted 6-fold coordination with V^{5+}−O−Me bridges bonds (Me = Mo^{5+} and/or Mo^{6+}).

The Te atoms should show an oxidation state of +4 as has been proposed in $TeMo_5O_{16}$[14,15] and in related MoVTe oxides.[8] The formation of Te^{4+} from Te^{6+} is generally accepted when the samples are calcined at high temperature.[22]

On the other hand, although the existence of V^{4+} cannot be completely ruled out (600−750-nm region) its presence, if any, should be very low. From these results, it can be concluded that Mo^{6+}, Mo^{5+} (≈20%), V^{5+}, and Te^{4+} are the oxidation states in $Te_{0.33}Mo_{0.75}V_{0.25}O_x$. This is in agreement with the oxidation state previously proposed for Mo and Te in $TeMo_5O_{16}$[20] and for Mo, V, and Te in related MoVTe-based materials.[8]

Taking into account the above information, the microstructural study by means of electron diffraction (SAED) and electron microscopy (HREM) was performed to establish the possible order−disorder situations associated with the presence of both Mo and V in the hexagonal bronze skeleton of the structure.

Figure 3a corresponds to the electron diffraction pattern along the [001] zone axis. Besides the stronger reflections consistent with the previously described hexagonal cell, extra diffraction maxima appear doubling the [100], [010], and [1$\bar{1}$0] reciprocal directions. The extra diffraction spots therefore define double cell dimensions in the *ab* plane, that is, 0.145 nm. The corresponding electron micrograph is shown in Figure 3b. The basic contrast variation in the image can be related to the hexagonal disposition of hexagonal tunnels formed by the M cations (M = Mo, V) characteristic of the HTB structure. However, different areas in the crystals can be observed which show a superimposed contrast doubling the [100], [010], or [1$\bar{1}$0] directions. The appearance of the three different areas simultaneously in the same crystal gives rise to the diffraction pattern shown in Figure 3a. When the 2-fold superstructure appears only along one of the above-mentioned directions, the electron diffraction pattern of Figure 4 is obtained, indicating that the new unit cell is, in fact, of orthorhombic symmetry (parameters $a \approx 0.128$ nm and $b \approx 0.73$ nm).

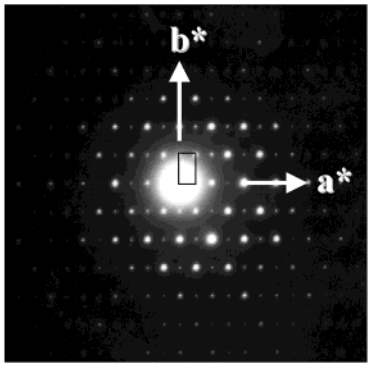

Figure 4. SAED pattern taken along the [001] zone axis, where the superstructure is only patent along one direction. The projection of the new reciprocal lattice has been marked.

Figure 5a corresponds to the [100] reciprocal lattice projection. The absence of superstructure maxima along [001]* indicates that there is no extra order with respect to the HTB structure, along this direction (thus, $c \approx 0.4$ nm). Figure 5b shows the HREM image corresponding to the same projection. The homogeneous contrast variation is in agreement with the previous statement.

From the above results, we can describe the crystals as being formed by structural domains of an orthorhombically distorted unit cell derived from the HTB-type structure, which appear separately or coherently intergrown at 60° (see Figure 3b). This relative assembly would justify the SAED patterns shown in Figure 3a and the apparently double unit cell, parameter $a \approx 0.145$ nm. The occurrence of only one type of such domains gives rise to diffraction patterns as the one shown in Figure 4. At this point, it is worth mentioning that all the microstructural features reported above are

(21) Hanke, W.; Bienert, R.; Jerchkewitz, H. G. *Z. Anorg. Allg. Chem*. **1975**, *414*, 109.
(22) Janssen, F. J. G. *J. Therm. Anal.* **1991**, *87*, 1281.

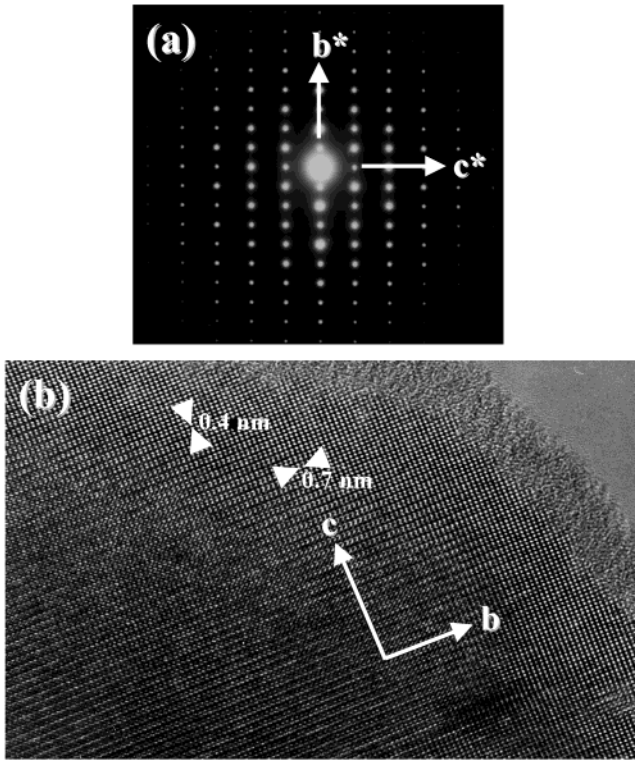

Figure 5. (a) SAED pattern corresponding to the [100] reciprocal projection. (b) HREM image taken along the same projection.

also observed when niobium is partially substituting molybdenum and vanadium in the HTB skeleton,[23] indicating the formation of a solid solution.

The microstructural characterization results led us to relate the new superstructure found with an ordered distribution of molybdenum and vanadium in the framework of the HTB-type structure. A careful chemical analysis of the crystals by means of X-ray microanalysis showed that there were no local deviations from the average composition previously determined. This observation together with the small difference in ionic radii among vanadium (V), molybdenum (V), and molybdenum (VI) in octahedral coordination allowed us to eliminate the ordered disposition of Mo and V in the structural framework, as the probable origin of the superstructure observed. This is reinforced by the fact that there are no microstructural differences when niobium is incorporated into the structural framework, as we have mentioned above.

When considering the anionic sublattice as the origin of the superstructure, one question arises. The DR spectrum suggests that only a quantity of Mo around 20% is in the form Mo(V) and there is no evidence about the presence of V(IV) ions. Moreover, provided that only Te^{4+} is present, the oxygen content must be close to $O_{3.4}$. The theoretical oxygen content of the crystal structure to which it should be compared can take two different values slightly differing as a function of the local environment of tellurium. This can be a trigonal pyramid TeO_3 (like Sb in $Sb_2Mo_{10}O_{31}$[24]) or a trigonal bipyramid TeO_4 (like in the orthorhombic form of $TeMo_5O_{16}$[15]). In the first case, it should correspond to the $O_{3.16}$ anionic composition and in the second case to $O_{3.33}$. This last composition is in agreement with the experimental value and thus one can assume there are no oxygen vacancies in the structure. Therefore, the possibility of extra order in the anionic sublattice has to be ruled out.

The location of tellurium is worth noting. From the above discussion, it seems that the Te atoms should be linked to each other by oxygen atoms, forming infinite chains along the hexagonal tunnels. The coordination polyhedron of Te is a trigonal bipyramid [TeO_4E] with four oxygen atoms and the lone pair E pointing at the center of the tunnel. The resulting off-center disposition

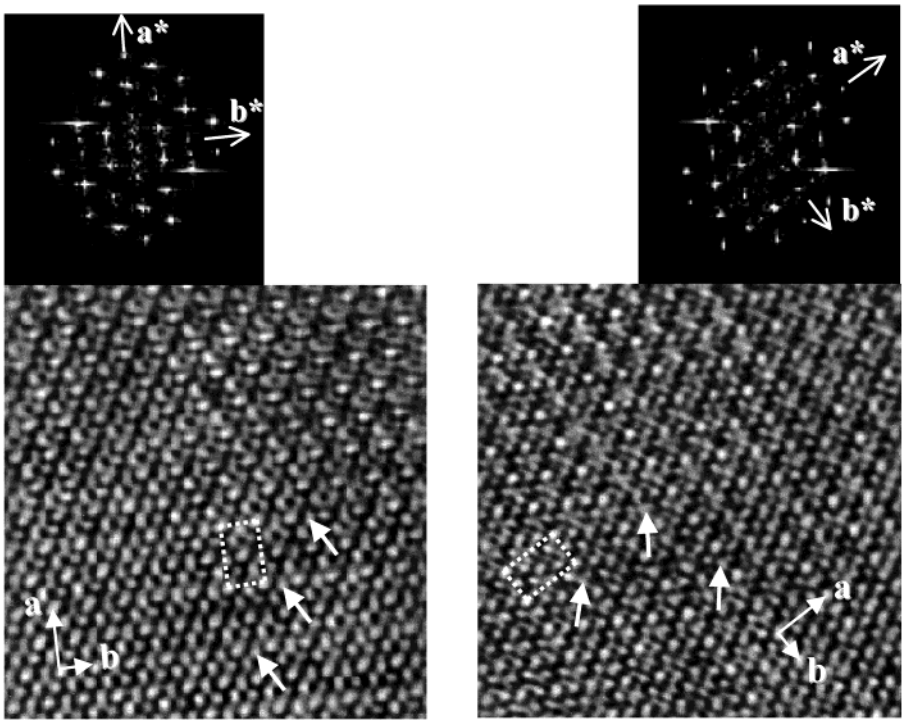

Figure 6. Enlarged HREM images corresponding to two different areas of a crystal in the [001] reciprocal projection. Optical diffraction patterns have been included to show the superstructure reciprocal directions.

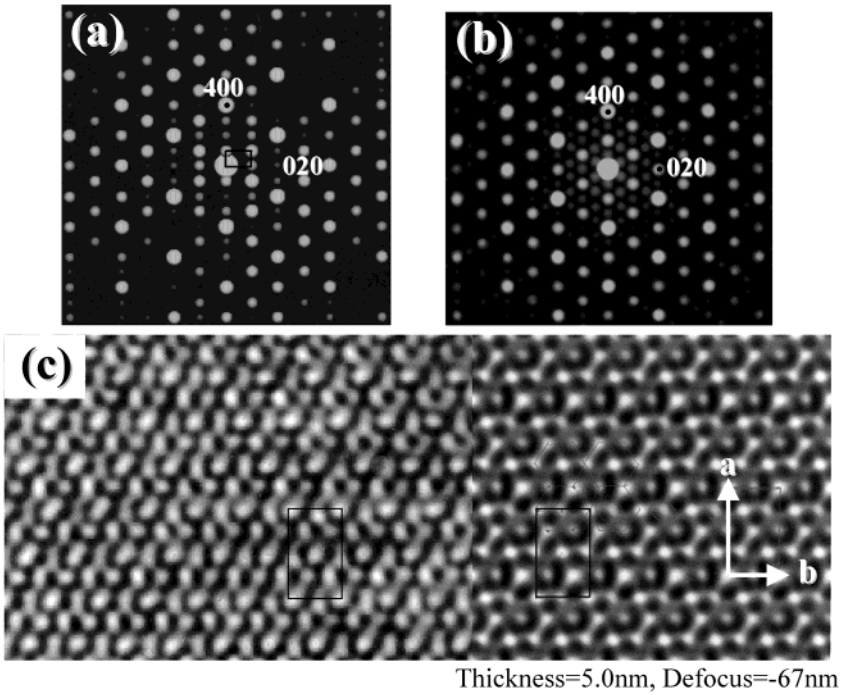

Figure 7. (a) Simulated SAED pattern in the [001] projection. (b) Overlapping of the diffraction effects in the three independent reciprocal directions [100], [010], and [1$\bar{1}$0]. (c) Experimental and simulated images on the [001] projection.

of tellurium atoms is, therefore, an important structural feature of this crystal phase when compared with the traditional hexagonal tungsten bronzes described by Mágneli.[17] This asymmetric location of tellurium can be observed in the corresponding high-resolution electron micrograph. Figure 6 shows two enlarged areas of the same crystal in the [001] projection, which have been taken in the thin edge of the crystal. These areas have been chosen because of the mutual orientation of the superstructure observed on them. The projected unit cell has been marked on both images. White spots have been interpreted as projected columns of heavy metal atoms. The arrows mark a ring of six white spots; these contrast features are assigned to six MO_6 octahedra linked by corners to form a six-membered ring, which creates a six-sided tunnel. The off-center Te location can be appreciated. In these micrographs, deviation of the tellurium atoms from the central position of the hexagonal tunnels occurs in two of the three possible directions, to satisfy the trigonal bipyramid coordination environment.

Projected atomic coordinates for the metal atoms (Mo/V, Te) have been determined from different HREM images and the average values have been used to simulate the superstructure observed. Estimation of the metallic positions is influenced by an error mainly due to the limited resolution of the data (≈0.25 nm) and to the fact that only data from the *(hk*0) projection were used. Oxygen atoms were located on the positions of the HTB Mágneli phase.[17] No symmetry restrictions have been imposed. Figure 7a corresponds to the simulated SAED pattern in the [001] projection. Extra diffraction maxima appear doubling the [100] reciprocal direction. A 60° clockwise tilt of the diagram would give rise to double periodicity along [010], and after a second tilt of 60°, the [1$\bar{1}$0] direction would be doubled as well. Overlapping of these three effects results in the diagram shown in Figure 7b, and the agreement with the experimental SAED pattern (Figure 3a) is clear. Figure 7c shows the agreement between the experimental and the calculated image (conditions: thickness = 5.0 nm; defocus = −67 nm).

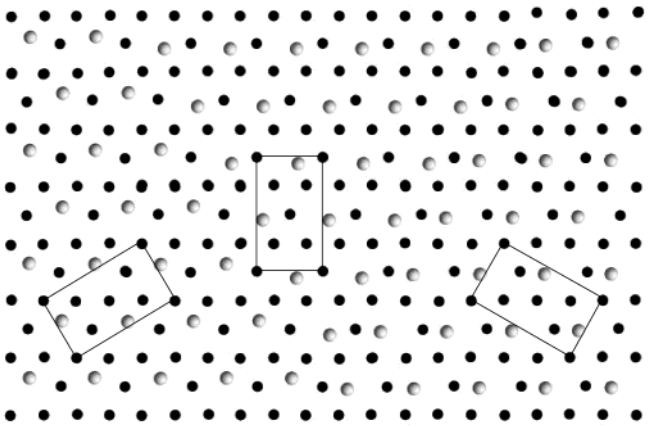

Figure 8. Schematic drawing of the proposed model. Oxygen atoms have been omitted for simplicity. Representation includes domains in the three possible orientations. The unit cells have been drawn inside each domain to enhance the double periodicity along the three directions.

Crystals of this new phase should therefore be constituted by such domains in a similar way than that modeled in Figure 8. The structure model representation supposes a simplification of the real situation in the sense that inside each domain every tellurium atom is considered to move out of the center of the hexagonal tunnel, not only in the same direction but also with the same magnitude. A more realistic situation would be to consider the fact that an octahedral constituting the structural framework is occupied by both molybdenum

(23) Botella, P.; Garcia-González, E.; González-Calbet, J. M.; López Nieto, J. M.; Solsona, B., to be published.
(24) Parmentier, M.; Gleitzer; C.; Courtois, A.; Protas, J. *Acta Crystallogr. B* **1963**, *35*, 1979.

and vanadium (and/or niobium), thus probably leading to different displacements of Te atoms, although in one unique direction. In this last case, the unit cell would be a primitive cell and the superstructure reflections would be allowed reflections. In the first case, the unit cell would be a centered cell and, therefore, the extra diffraction maxima would be forbidden reflections appearing only due to double-diffraction phenomena. The experimental diffraction patterns do not show any systematic extinction concerning the *(hkl)* reflections with $h + k = 2n + 1$. In contrast, the simulated SAED patterns do show such extinctions except when the crystal thickness is enough to allow them to appear as due to the double-diffraction effect. This is consistent with the above discussion in which the simulated diagrams have been obtained from the average atomic coordinates from the HREM images and, therefore, no difference has been considered between octahedral positions occupied by molybdenum or vanadium. The displacement for every atom in the Te sublattice is equivalent inside one domain and it results in a *C* centered cell.

In summary, we have presented a structural investigation of the new $Te_{0.33}(Mo,V)O_{3.33}$ bronze. Microstructural characterization has been carried out, as the first step in elucidating the role of this new orthorhombic phase in the effectiveness of catalysts.

Acknowledgment. Financial support from DGICYT in Spain through Projects PPQ2000-1396 and MAT2001-1440 is gratefully acknowledged. Authors are also grateful to the Centro de Microscopía Electrónica (U.C.M.) for facilities.

CM021223M